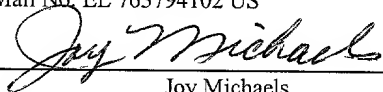


I hereby certify that this correspondence and any attachments are being deposited with the United States Postal Service as Express Mail on August 21, 2001, in an envelope addressed to: Box Patent Application, Assistant Commissioner for Patents, Washington, D.C. 20231.

Express Mail No. EL 763794102 US



Joy Michaels

UNITED STATES PATENT APPLICATION

For

DISTRIBUTED BRAGG REFLECTORS INCORPORATING SB MATERIAL FOR LONG-WAVELENGTH VERTICAL CAVITY SURFACE EMITTING LASERS

INVENTORS: LARRY A. COLDREN
SANTA BARBARA, CA
USA CITIZEN

ERIC M. HALL
SANTA BARBARA, CA
USA CITIZEN

GUILHEM ALMUNEAU
ACSCH BEI BIRMENSdorf, ZH
SWITZERLAND
FRENCH CITIZEN

OPPENHEIMER

OPPENHEIMER WOLFF & DONNELLY LLP
2029 Century Park East, Suite 3800
Los Angeles, California 90067-3024
(310) 788-5000
Fax (310) 788-5100

Attorney Matter No. 510015-265
Drawings: 12 sheets

DISTRIBUTED BRAGG REFLECTORS INCORPORATING SB MATERIAL FOR LONG-WAVELENGTH VERTICAL CAVITY SURFACE EMITTING LASERS

[0001] This invention was made with the support of the United States Government under Grant No. MDA972-98-1-0001, awarded by the Department of Defense (DARPA). The Government has certain rights in this invention under 35 U.S.C. §202

[0002] The contents of this application are related to those provisional applications having serial numbers 60/227,165, 60/227,161, and 60/226,866, filed August 22, 2000, and a provisional application having serial number 60/262,541, filed January 16, 2001. The present application claims priority to these related provisional patent applications and their contents are hereby incorporated by reference in their entirety into the present disclosure. The contents of this application are also related to several nonprovisional patent applications being filed concurrently herewith. These nonprovisional patent applications are hereby incorporated by reference in their entirety and have the following attorney docket reference numerals: 510015-263, 510015-264, 510015-265, 510015-266, 510015-268, 510015-269, 510015-270, 510015-271, and 510015-272.

BACKGROUND OF THE INVENTION

[0003] *1. Field of the Invention:*

[0004] The invention relates in general to a vertical cavity surface emitting laser (VCSEL). More particularly, the invention relates to growth methods and structures for distributed Bragg reflectors (DBRs) utilized in VCSELs.

[0005] *2. General Background and State of the Art:*

[0006] Semiconductor lasers are widely used in optical applications, in part because semiconductor fabrication techniques are relatively inexpensive and yield reliable, consistent results. Also, they are easily packaged into current microelectronics. A relatively new class of semiconductor lasers, vertical cavity surface emitting lasers (VCSELs), has been developed through the evolution of this technology. Unlike conventional edge emitting lasers that emit light in a direction parallel to the semiconductor substrates where the lasers are formed, VCSELs have optical cavities

perpendicular to the substrate, and thus emit optical radiation in a direction perpendicular to the substrate. In addition to various performance and application-adaptable improvements created thereby, VCSELs simply require reduced complexity in their fabrication and testing, as compared to conventional edge emitting semiconductor lasers.

[0007] Vertical cavity surface emitting lasers (VCSELs) have been proven to be solutions for low-cost transmitters for high-speed data communications at 980nm and 850nm and have shown great potential for cost-effective telecommunication systems at longer wavelengths as well, such as 1.55 μ m and 1.3 μ m. These long wavelength VCSELs will satisfy increasing demand for high speed data transmission over tens of kilometers. 10-Gigabit Ethernet is one example, which requires inexpensive transmitters with a data rate of 10G bit per second (Gbps) and up to 40km reach over single-mode fiber.

[0008] VCSELs are semiconductor lasers having a semiconductor layer of optically active material, such as gallium arsenide or indium gallium arsenide or the like, sandwiched between highly-reflective layers of metallic material, dielectric material, epitaxially-grown semiconductor dielectric material or combinations thereof, most frequently in stacks. These stacks are known as distributed Bragg reflectors, or DBRs. DBRs are used to reflect emitted light back into the active material of a VCSEL. As is conventional, one of the mirror stacks is partially reflective so as to pass a portion of the coherent light built up in the resonating cavity formed by the mirror stack/active layer sandwich. Laser structures require optical confinement and carrier confinement to achieve efficient conversion of pumping electrons to stimulated photons (a semiconductor may lase if it achieves population inversion in the energy bands of the active material.)

[0009] The development of vertical-cavity surface-emitting lasers (VCSELs) at the telecommunications-important wavelength of 1.55 μ m has been hindered by the absence of a substrate that is suitable for both technologically-developed distributed Bragg reflectors (DBRs) and quantum well active regions. In fact, despite the demonstration of VCSELs grown on a single substrate, the best results have been obtained through the fusion of InP-based active regions and AlGaAs-based DBRs.

[0010] To overcome mirror limitations on InP, several groups have examined AlGaAsSb-based DBRs, which have a refractive index contrast that is similar to AlGaAs-based DBRs at this wavelength. The high index contrast leads to a lower penetration depth than traditional InGaAsP-based DBRs and, therefore, implies lower optical loss in the structure. Only optically-pumped VCSELs using such DBRs, however, have been demonstrated.

[0011] While both short wavelength and long wavelength VCSELs have proven to offer excellent solutions for many applications in the evolving optical applications marketplace, they also have certain limitations and drawbacks that are well known in the art. Some of these drawbacks are inherent to the conventional materials used in the fabrication of Bragg mirrors for VCSELs grown on InP substrates. For example, the accuracy and reproducibility of an As, Sb composition in a AlGaAsSb semiconductor system is very difficult to achieve in DBR fabrication. While such materials have conventionally been considered and used as the best selection for the mirrors, they do not effectively optimize high reflectivity, good electrical conduction and low thermal resistance.

INVENTION SUMMARY

[0012] The present invention provides a method of growing a distributed Bragg reflector for use in a VCSEL using molecular beam epitaxy. The present invention also provides a method of fabricating a distributed Bragg reflector (DBR) in which the amount of particular semiconductor materials used in the DBR are controlled in the molecular beam epitaxy process.

[0013] The present invention provides a DBR for use in vertical cavity surface emitting laser (VCSEL) having an Sb-based semiconductor material. The present invention further provides a method of enhancing thermal properties in a DBR by growing AlGaAsSb layers and InP layers on a substrate to form the DBR. A method of fabricating DBRs using these two types of layers is also provided.

[0014] One aspect of the present invention provides a method for controlling material composition in a distributed Bragg reflector. The method includes applying reflection high-energy electron diffraction (RHEED) oscillations in molecular beam epitaxy to a substrate, measuring the intensity of antimony (Sb) atoms present in the substrate in

response to the RHEED oscillations, and calibrating the amount of Sb to be incorporated into the substrate, with the amount depending upon the frequency of the RHEED oscillations induced by the Sb atoms.

[0015] Accordingly, one object of the present invention is to provide a method of controlling material composition in a distributed Bragg reflector for use in a VCSEL. It is another object of the present invention to provide a method of fabricating a distributed Bragg reflector for use in a VCSEL incorporating the above method of controlling material composition. It is still another object of the present invention to provide a VCSEL and method of fabrication of a VCSEL which enhances the thermal and reflective characteristics of the VCSEL.

BRIEF DESCRIPTION OF THE DRAWINGS

[0016] FIG. 1 is a flowchart overview of the process of forming a DBR using one embodiment of the present invention;

[0017] FIG. 2 is a plot of the intensity of RHEED oscillations over time when induced by Sb atoms on a substrate;

[0018] FIG. 3 is a diagrammatic representation of atoms on a substrate during standard molecular beam epitaxy;

[0019] FIG. 4 is a diagrammatic representation of atoms on a substrate during mixed group V molecular beam epitaxy;

[0020] FIG. 5 is a plot of Sb composition in GaAsSb, AlAsSb, and GaAsSb layers as a function of calibrated incorporation rates of Sb normalized with the incorporation rate of Ga;

[0021] FIG. 6 is a plot of the room-temperature photoluminescence spectra of AlGaAsSb/AlAsSb DBRs and AlGaInAs/AlAsSb DBRs;

[0022] FIG. 7 is a schematic representation of a VCSEL having an Sb-based DBR;

[0023] FIG. 8 is an additional schematic representation of a VCSEL having showing Sb-based DBRs of specific periods;

[0024] FIG. 9 is a plot of L-I and I-V for a VCSEL having an etched pillar of 25 μ m

[0025] FIG. 10 is a schematic representation of a VCSEL with a DBR having an AlGaAsSb/InP material composition;

[0026] FIG. 11 is a flowchart overview of the process of forming a DBR using InP;

[0027] FIG. 12 is a plot of differences in band alignment between arsenide-antimonide (AsSb) alloys and InP;

[0028] FIG. 13 is a plot of current density versus voltage characteristics of an Al_{0.1}GaAsSb/InP DBR in a growth direction;

[0029] FIG. 14 is a table of thermal conductivity measurements of AsSb compounds in bulk layers and in DBRs; and

[0030] FIG. 15 is a plot of calculated and experimental spectra of a 20.5 period AlGaAsSb/InP DBR.

DETAILED DESCRIPTION OF THE EMBODIMENTS

[0031] FIG. 1 is a flowchart describing the process of growing a DBR in one embodiment. Block 12 shows the step of providing a substrate on which DBR materials are grown. Block 14 shows the step of growing semiconductor material on the substrate. As described herein, molecular beam epitaxy is used in this embodiment to grow the materials on the substrate. Block 16 shows the step of observing RHEED oscillations to monitor the composition of group V elements such as antimony (Sb) in the semiconductor material. The RHEED oscillations occur simultaneously as semiconductor material is being grown on the substrate. Growth continues as measurements are taken of the RHEED oscillations.

[0032] The RHEED oscillations are used to monitor the amount of a group V element's atoms being to the substrate. Block 18 shows the next step, in which measurements of the oscillation frequencies are taken and used to control the amounts of the group V elements incorporated into the semiconductor material. Additionally, the RHEED oscillations are used to monitor the amount of group III elements such as Ga. A valve or other control mechanism, such as temperature, is used to control the rate of Sb reaching the substrate. Frequencies of the RHEED oscillations indicate the valve setting to control the composition rate of Sb. Block 20 shows the step of calibrating the amount

of group V element-based material based upon the measurements taken in Block 18 and as described herein.

[0033] As semiconductor materials are being applied to the substrate, Ga and Sb are simultaneously hitting the substrate. However, because it is desirable to control the amount of Sb (or another similar group V element such as arsenic (As)), the flow of Sb must be monitored. Beginning with a condition in which there are fewer Ga atoms on the substrate than there are Sb atoms, oscillations registering a frequency change will occur when the amount of Ga atoms exceeds the amount of Sb atoms. Because it is the incorporation rate of the group V, or Sb atoms that are being controlled, a shutter is used to limit the flow of Ga atoms to the substrate when Ga atoms begin to exceed Sb atoms, since too many Ga atoms can swamp the process of accurately controlling Sb composition. This step of controlling the amount of Ga atoms hitting the substrate is shown in Block 22 of FIG. 1. This process of determining valve settings for proper Sb incorporation rates, and controlling the flow of Ga atoms to measure the frequency of oscillations, repeats until an appropriate composition rate of Sb has been reached.

[0034] In the present invention, all the growths of arsenide-antimonide compounds on InP substrates have been made using calibrations at a substrate temperature of 470°C. The composition of Sb in the $\text{Al}_x\text{Ga}_{1-x}\text{As}_{1-y}\text{Sb}_y$ layers is set with regard to the total group-III growth rate. The modifications of growth rates according to the different atoms surface density between GaAs, GaSb and InP are also contemplated, since the calibrations were done on GaAs and GaSb, and the grown layer has the same lattice as InP. In order to maintain a V/III ratio higher than unity, the As flux is always slightly higher than the calibrated value for 1-y As composition.

[0035] FIG. 2 is a plot of frequencies of group-V induced reflection high-energy electron diffraction (RHEED) oscillations used to monitor the incorporation of Sb and As in ternary compounds GaAsSb and AlAsSb as well as the quaternary compound AlGaAsSb. The calibration of the group-V composition is achieved by correlating the Sb incorporation rate with beam equivalent pressure (BEP). An equivalent in situ technique using gas-source molecular beam epitaxy (MBE) is also used to control the group-V compositions of InGaAsP alloys.

[0036] Substrate growths are performed in an MBE system equipped with solid source cracking effusion cells producing As_2 and Sb_2 species on the surface. Conventional RHEED oscillations of group-III species under As_2 overpressure are applied on a GaAs substrate to calibrate the growth rates. The Sb and As incorporation rates have been measured also by RHEED oscillations while maintaining an overpressure of Ga during the growth. When an excess of the group-III element is formed at the surface, for example by growth using a high III/V flux ratio, the oscillation period corresponds to the growth of a monolayer, but it is not related to the group-III element flux. Instead it relates to the group-V flux as a product of this flux and the sticking coefficient of the group-V element. The As-induced oscillations have been observed on GaAs layers, and on the same substrate the Sb-induced RHEED oscillations have been performed on a thick totally smooth GaSb layer. FIG. 2 shows an example of such Sb-induced RHEED oscillations at a substrate temperature of 420°C . Before $t = 1.5$ s the surface is under Sb flux, and at $t = 1.5$ s the Ga shutter is opened. The behavior of the RHEED intensity is characteristic of a group-III stabilized surface: the specular beam brightness drops rapidly during the first few monolayers and oscillates with a shorter period than the following Sb-induced oscillations. At $t = 4$ s the oscillations caused by the Sb atoms begin while being rapidly damped due to the degradation of the Ga-stabilized surface.

[0037] Molecular beam epitaxy is a method of growing high-purity epitaxial layers of compound semiconductors. It has evolved into a popular technique for growing group III-V compound semiconductors as well as several other materials. MBE can produce high-quality layers with very abrupt interfaces and good control of thickness, doping, and composition. Because of the high degree of control possible with MBE, it is a valuable tool in the development of sophisticated electronic and optoelectronic devices.

[0038] In MBE, the constituent elements of a semiconductor in the form of "molecular beams" are deposited onto a heated crystalline substrate to form thin epitaxial layers. The "molecular beams" are typically from thermally evaporated elemental sources, but other sources include metal-organic group III precursors (MOMBE), gaseous group V hydride or organic precursors (gas-source MBE), or some combination (chemical beam epitaxy or CBE). To obtain high-purity layers, it is critical that the material sources be extremely pure and that the entire process be done in an ultra-high vacuum environment. Another important feature is that growth rates are typically on the order of

a few Å/s and the beams can be shuttered in a fraction of a second, allowing for nearly atomically abrupt transitions from one material to another.

[0039] Calibration of the growth rate is essential for the proper tuning of resonant-cavity devices. There are several *in-situ* techniques which can be used in MBE. One way to measure the growth rate is to use the BEP gauge. This measurement is dependent on factors such as the geometry of the system and ionization efficiency of the material being measured, but for a given system and material, the BEP reading is proportional to the flux at the sample surface and hence the growth rate. Unlike other techniques, a BEP measurement does not require that any epitaxial layers be grown. Growing epitaxial layers requires an approximate knowledge of the flux beforehand, so the BEP is particularly useful for effusion cells which are being used for the first time. For the Varian Gen II, a BEP reading in the mid to high 10^{-7} Torr range gives Ga growth rates of about $1 \mu\text{ m/hour}$. However, the technique is not a direct measure of the growth rate, so some other *in-situ* or *ex-situ* technique must still be used to relate the BEP to a growth rate.

[0040] One such technique includes RHEED intensity oscillations, which are used as an accurate, quick, direct measure of the growth rates in MBE. When growth is initiated on a smooth GaAs surface, the intensity of the RHEED pattern, especially the specular reflection, starts to oscillate. The oscillation frequency corresponds to the monolayer growth rate, where a monolayer (ML) is the thickness of one full layer of Ga and one full layer of As atoms. When a layer starts it is smooth and the specular spot is bright, but as the layer nucleates, islands form on the surface, and the specular spot dims. As the layer finishes, the islands coalesce into a flat layer, and the specular spot intensity increases. The oscillation of the specular spot intensity has been attributed to the oscillating roughness of the layers changing the diffuse scattering, but the incident angle dependence of the oscillations suggest that interference between electrons scattering from the underlying layer and the partially grown layer contribute to these oscillations.

[0041] FIG. 3 and FIG. 4 are diagrammatic representations of atoms 26 on a substrate. FIG. 3 shows the atoms 26 during standard molecular beam epitaxy, while FIG. 4 shows the atoms 26 during mixed group V molecular beam epitaxy including Sb atoms 28. MBE typically utilizes group V overpressure and assumes that all group III

elements will stick. However, when two group V elements (such as As and Sb) are included in the overpressure, the composition must be determined as described herein.

[0042] FIG. 5 is a plot showing the resulting Sb composition measured in GaAsSb, AlAsSb and AlGaAsSb layers grown on InP as a function of the Sb incorporation rate calibrated as described above. Some of these layers are near to InP lattice-matched compositions ($x_{\text{sb}} \approx 0.5$) and other growths were performed with $x_{\text{sb}} \approx 0.8$. Over the whole composition range the experimental Sb composition depends linearly on the normalized Sb flux as $y \approx x$. The mean deviation of Sb composition from the fit is 0.0186 (maximum deviation = 0.039). The best linearly dependent fit can be obtained with $y = 1.4x$ and a mean deviation of 0.0095 (maximum deviation = 0.02).

[0043] In order to demonstrate the good quality of the AlGaAsSb layers, two DBRs containing 10.5 periods of $\text{Al}_{0.2}\text{Ga}_{0.8}\text{AsSb}/\text{AlAsSb}$ were grown on InP. The main difference between the mirrors is that one was grown with $\text{Al}_{0.2}\text{GaAsSb}$ quaternary bulk layers and the other with a digital-alloy $(\text{AlAsSb})_{0.2}(\text{GaAsSb})_{0.8}$. By using such digital alloys we can eliminate growth pauses at each mirror interface because of group-III cell temperature changes when only one Al cell is available on the MBE system. FIG. 6 is a plot of photoluminescence measurements at room temperature performed on both AlGaAsSb/AlAsSb DBRs and AlGaInAs/AlAsSb DBRs. The signals measured for AlGaAsSb in the mirrors are very intense but the digital quaternary alloy shows more intensity than the analog AlGaAsSb. The full-widths at half maximum are respectively 65 meV for the digital quaternary alloy and 54 meV for the analog one. As a comparison the photoluminescence signal observed for a 10.5 periods Be-doped AlGaInAs/AlAsSb is also depicted in FIG. 6. The wavelength at the maximum of both peaks is 1222 nm which corresponds to the calculated band-gap wavelength of $\text{Al}_{0.17}\text{Ga}_{0.83}\text{AsSb}$ close to the 20% Al expected.

[0044] FIG. 7 is a schematic representation of another aspect of the present invention, in which an electrically-pumped, Sb-based vertical-cavity laser 30 operating at 1.55 μm is produced in a single epitaxial growth. The laser 30 employs AlGaAsSb DBRs 32 and 34 and an AlInGaAs-based active region 36, and has a room temperature threshold current density of 1.4 kA/cm^2 and an external quantum efficiency of 18%. The DBRs 28 and 30 employ a plurality of layers of semiconductor material, each alternating

layer having the material composition of AlGaAsSb. In another embodiment, the DBRs 28 and 30 have a plurality of layers of semiconductor material, only one of which includes the element antimony (Sb).

[0045] The VCSEL 30 is grown by a molecular beam epitaxy on an *n*-doped (Sn) InP substrate 38. The active region 36 includes a 1λ cavity in which five strain-compensated AlInGaAs quantum wells are grown. A thin, heavily-doped tunnel junction 40, using CB_{r4} as the *p*-type dopant and Si as the *n*-type dopant, is placed at a standing-wave null of the mode to provide electron-hole conversion from the top *n*-DBR.

[0046] FIG. 8 is a schematic representation of one embodiment of the present invention in which the bottom DBR 34 includes 23 pairs of $\text{AlAs}_{0.56}\text{Sb}_{0.44}$ and $\text{Al}_{0.2}\text{Ga}_{0.8}\text{As}_{0.58}\text{Sb}_{0.42}$ $\lambda/4$ -layers lattice-matched to InP. The calculated reflectivity for this mirror is 99.6%. The top DBR 32, which has a calculated reflectivity of 99.9%, includes 30 periods of the same material combination plus a phase-matching layer for a metal contact 42. Both DBRs 32 and 34 have linearly graded interfaces between the low- and high-index layers and are uniformly *n*-type doped with the donor tellurium (Te) using PbTe ($n \cong 10^{18}/\text{cm}^3$ in AlAsSb). Two *n*-type DBRs are chosen to reduce both the voltage drop and optical losses in the VCSEL.

[0047] In general the DBRs 32, 34 can include alternating layer pairs of $\text{Al}_a\text{Ga}_{1-a}\text{As}_b\text{Sb}_{1-b}$ which are approximately lattice-matched to InP. The subscript “a” can be greater than 0.9 in one layer of the alternating layer pairs and less than 0.3 in the other layer of the alternating layer pairs. In the higher-index layers with “a” less than 0.3, “a” should still be large enough such that the layer is substantially transparent to lasing light. Here “b” can be a positive number and preferably greater than approximately 0.5.

[0048] More specifically, the DBRs 32, 34 can consist, respectively, of preferably twenty-three and thirty-two pairs of $\text{Al}_{a1}\text{Ga}_{1-a1}\text{As}_x\text{Sb}_{1-x}$ and $\text{Al}_{a2}\text{Ga}_{1-a2}\text{As}_x\text{Sb}_{1-x}$ ($a1 > 0.9$, $a2 < 0.3$, $x > 0.5$) $\lambda/4$ -layers, lattice-matched to the InP cladding layers. Lattice-matching is achieved by using previously-calibrated group-V induced reflection high-energy electron diffraction oscillations and then growing at conditions with near-unity antimony incorporation rates. As an alternative, only the top cladding layer or the bottom cladding layer may be present in the VCSEL. A small amount of Ga is generally added to the

AlAsSb reflecting surfaces so as to stabilize these surfaces chemically, and make them more resistive to degradation without substantially increasing their index of refraction.

[0049] The cavity mode has a reflectivity spectrum of 1.55 μm measured after growth, which is centered on a > 140 nm stopband (reflectivity $> 99\%$). Other embodiments can have an approximate range between 1.3 and 1.6 microns. The top DBR 32 is then removed in order to examine the photoluminescence (PL) of the quantum wells. The PL peak is at ~ 1580 nm, placing the cavity mode on the broad, short-wavelength shoulder of the PL spectrum. The mode and PL peak can be aligned by lowering the operation temperature.

[0050] Pillars with diameters ranging from 10 to 100 μm are then fabricated by reactive ion etching using the top metal contact as an etch mask. Contacts may also be deposited on the substrate 38 backside.

[0051] FIG. 9 is a plot of the $L-I$ and $I-V$ results from a VCSEL having a 25 μm diameter pillar operated in pulsed-mode at room temperature. The threshold current is 7 mA, corresponding to the current density of 1.4 kA/cm^2 . The external differential quantum efficiency of this device was 18% and the maximum power was 2 mW. Lasing is achieved up to 45°C with a threshold current of 15.5 mA.

[0052] FIG. 9 also shows that the devices exhibit a high voltage that most likely is attributable to both a high contact resistance in this processing run and to the DBRs which have a relatively low doping level. By increasing the doping a few periods away from the cavity or by using intra-cavity contacts, it is anticipated that this voltage drop may be reduced significantly without introducing additional optical losses.

[0053] In accordance with another aspect of the present invention, FIG. 10 is schematic representation of a VCSEL 44 having DBRs 46 including InP and AlGaAsSb respectively as low-refractive index and high-refractive index quarter-wavelength layers. The DBRs 46 have alternating layers of semiconductor material, where one layer is AlGaAsSb and the next layer is InP. The introduction of InP layers in the DBRs 46 leads to numerous benefits such as easier epitaxial growth of a binary alloy, and intrinsic low thermal resistivity and high electrical conductivity of the InP material. In particular, InP has the unique property of combining a low refractive index ($n = 3.17$) and a direct bandgap in the near-infrared ($E_T \equiv 0.92 \mu\text{m}$). For the 1.55 μm DBRs, this avoids carrier

transfers between Γ and X valleys, existing with other low refractive index materials (AlAsSb and AlInAs).

[0054] In one embodiment, the DBRs 46 include 2l pairs of $\text{Al}_{0.1}\text{Ga}_{0.9}\text{As}_{0.52}\text{Sb}_{0.48}/\text{InP}$ N-doped with tellerium (Te) at approximately $3 \times 10^{18} \text{ cm}^{-3}$. This value was obtained from a Hall measurement on the DBR itself, grown on a semi-insulated (SI) InP substrate, and reflects an effective doping level because of the different activation efficiencies between the quaternary alloy and InP. The DBRs are grown by solid source molecular beam epitaxy (SSMBE) using valved cracker cells for As, Sb and P species. All the AlGaAsSb layers are nominally lattice-matched on InP.

[0055] For electrical characterizations, etched mesas defined by reactive ion etching (RIE) with a mixed flow of chlorine and argon were incorporated in the VCSEL. After etching, NiAuGe contacts were deposited in order to form transmission line model (TLM) test patterns.

[0056] FIG. 11 is a flowchart of steps in the process of fabricating a DBR 46 using this aspect of the present invention. Block 48 shows the step of providing a substrate on which a DBR structure will be grown. Block 50 shows the step of determining lattice-matching conditions for AlGaAsSb material. The lattice matching conditions are determined by observing and measuring RHEED oscillations on the substrate. Because the substrate and alternating layers of the DBR structure are composed of InP, which is a binary alloy having a static lattice constant, the primary concern in lattice matching the DBR layers is the composition of the elements in the AlGaAsSb layers of the DBR structure. Each of the elements of the AlGaAsSb structure has an influence on the overall lattice constant. Al and Ga (both group III elements) have a large effect on the refractive index, so their proportions are design selections for the DBR. Therefore, given a selected amount of the group III elements, the relative amounts of As and Sb, both group V elements, must be determined to match the lattice constant with that of the InP layers and substrate. RHEED oscillations are then observed and measured to determine proper proportions of As and Sb to arrive at the appropriate lattice constant to lattice match the AlGaAsSb layers to the InP layers and to the InP substrate.

[0057] Block 52 shows the step of growing a lattice-matched AlGaAsSb layer of semiconductor material on the substrate. AlGaAsSb layers are lattice-matched to both

the substrate and to the InP layers. Block 54 shows the step of growing an InP layer of semiconductor material on the substrate. Finally, Block 56 shows the step of doping the AlGaAsSb and InP layers on the substrate. The doping step occurs simultaneously with the growth of the AlGaAsSb and InP layers on the substrate, since dopants are introduced to the substrate as these semiconductor materials are being grown.

[0058] FIG. 12 is a plot of the differences in band alignment between arsenide-antimonide alloys and InP. The conduction band offset is quite important between AlAsSb and AlGaAsSb previously used. A drastic reduction of this offset can be achieved by substituting InP for AlAsSb. Another significant improvement is to avoid the scattering mechanisms encountered in the electron transport between direct and indirect bandgap materials. The InP/ $\text{Al}_{0.1}\text{Ga}_{0.9}\text{As}_{0.52}\text{Sb}_{0.48}$ heterostructure thus obtained is of type II, with a barrier height of 310 meV for the electrons. According to this, conduction band offset is higher than for InGaAsP/InP (186 meV) but lower than for AlGaInAs/AlInAs (381 meV).

[0059] Fig. 13 is a plot of the current density versus voltage characteristics of an $\text{Al}_{0.1}\text{GaAsSb/InP}$ DBR in the growth direction. As expected from the band diagram discussed above, the voltage drop is low; typically 10 mV per period is measured at a current density of 1 kA/cm^2 . From the modeling of the conduction band, depicted in the inset of the FIG. 13, the calculated thermionic component of the current leads to a voltage of 8 mV per pair. Again, if this result is compared to other systems used on InP, the voltage in AlGaAsSb/InP is the smallest. In an actual VCSEL structure including two AlGaAsSb/InP DBRs of 25 pair each, the total voltage due to the DBRs would be only 0.5 V.

[0060] FIG. 14 is a table of thermal conductivity measurements of AsSb compounds in bulk layers and in DBRs. Generally speaking, the only lattice-matched alloys to InP are ternary and quaternary alloys, and so their thermal conductivities are limited. This comes from the phonon scattering in a lattice with different atoms. The best way to maximize the thermal properties of a DBR is to use InP. In FIG. 14, the difference between InP and ternary or quaternary alloys is clearly demonstrated. An improvement of a factor two was obtained for InP-containing DBRs. By reasoning as an equivalent

electric circuit, one can deduce the relation between the thermal conductivities of the DBR and the constituting layers 1 and 2-as

[0061]
$$(d_1 + d_2)/K_{DBR} = d_1/k_1 + d_2/k_2$$

[0062] where d is the layer thickness and k the thermal conductivity.

[0063] The conductivity of the DBRs calculated from the experimental data of bulk layers is equal to the measured values, even for AlGaAsSb/AlAsSb or AlGaAsSb/InP. This indicates that phonon scattering occurs predominantly in the quaternary alloy rather than at the interfaces.

[0064] FIG. 15 shows the experimental and calculated reflectivity spectra. A good correlation is obtained for the high reflectivity stop-band and the higher wavelengths sidelobes. Whereas, at shorter wavelengths, we observe the incidence on the reflectivity curve of the AlGaAsSb absorption below the bandgap (E_T [Al_{0.1}Ga_{0.9}As_{0.52}Sb_{0.48}] \equiv 1.4 μ m). At the center-wavelength located at 1.47 μ m, the refractive index contrast used in the calculation was 1.135 with the refractive indices, $n = 3.61$ and $n = 3.18$, respectively for Al_{0.1}Ga_{0.9}As_{0.52}Sb_{0.48} and InP, leading to a maximum reflectivity of 0.994. One can also note the important width of the stop-band of about 100 nm.

[0065] It is to be understood that other embodiments may be utilized and structural and functional changes may be made without departing from the scope of the present invention. The foregoing descriptions of embodiments of the invention have been presented for the purposes of illustration and description. It is not intended to be exhaustive or to limit the invention to the precise forms disclosed. Accordingly, many modifications and variations are possible in light of the above teachings. For example, a distributed Bragg reflector according to the present invention may utilize alternating layers of semiconductor material having the element antimony, or it may utilize one layer of material having antimony in the mirror design. It is therefore intended that the scope of the invention be limited not by this detailed description.